Journal of Physics: Conference Series

PAPER • **OPEN ACCESS**

Periodic Solutions, Eigenvalue Curves, and Degeneracy of the Fractional Mathieu Equation

Journal of Physics: Conference Series **698** (2016) 012005 doi:10.1088/1742-6596/698/1/012005

Periodic Solutions, Eigenvalue Curves, and Degeneracy of the Fractional Mathieu Equation

A Parra-Hinojosa[1] and J C Gutiérrez-Vega[2]

[1] Department of Informatics, Technische Universität München. Boltsmannstr 3. Garching 85748, Germany

[2] Photonics and Mathematical Optics Group, Tecnológico de Monterrey, Monterrey 64849, México

E-mail: `juliocesar@itesm.mx`

Abstract. We investigate the eigenvalue curves, the behavior of the periodic solutions, and the orthogonality properties of the Mathieu equation with an additional fractional derivative term using the method of harmonic balance. The addition of the fractional derivative term breaks the hermiticity of the equation in such a way that its eigenvalues need not be real nor its eigenfunctions orthogonal. We show that for a certain choice of parameters the eigenvalue curves reveal the appearance of degenerate eigenvalues. We offer a detailed discussion of the matrix representation of the differential operator corresponding to the fractional Mathieu equation, as well as some numerical examples of its periodic solutions.

1. Introduction

There is an extensive literature dedicated to the Mathieu equation [1–3]

$$\left[\frac{\mathrm{d}^2}{\mathrm{d}t^2} + a - 2q\cos 2t\right]\Theta(t;q) = 0, \tag{1}$$

where $q \in \mathbb{R}$ is an equation parameter and $a \in \mathbb{C}$ is the eigenvalue (or characteristic number) of the equation. A classical problem associated with this equation is the determination of the eigenvalues $a(q)$ for which the solution $\Theta(t;q)$ is periodic in t.

Different forms of the Mathieu equation have also been studied, which include damping [4–7] and nonlinearities [8, 9], as well as quasi-periodic [10] and nonhomogeneous [11] forms.

In a recent paper, Rand et al. [12] investigated the fractional Mathieu equation

$$\left[\frac{\mathrm{d}^2}{\mathrm{d}t^2} + a - 2q\cos 2t + c \ {}_{-\infty}\mathrm{D}_t^{\alpha}\right]\Theta(t;q) = 0, \tag{2}$$

where $c \in \mathbb{R}$ is a constant and ${}_{-\infty}\mathrm{D}_t^{\alpha}$ denotes the Riemann-Liouville fractional derivative of order $\alpha \geq 0$ and lower limit $b = -\infty$ defined as [13]

$${}_{-\infty}\mathrm{D}_t^{\alpha} f(t) = \frac{1}{\Gamma(n-\alpha)}\frac{\mathrm{d}^n}{\mathrm{d}t^n}\int_{b=-\infty}^{t}\frac{f(\xi)}{(t-\xi)^{1+\alpha-n}}\mathrm{d}\xi, \qquad \alpha \geq 0, \tag{3}$$

with n being the smallest integer exceeding α. Rand et al. studied the case $\alpha \in (0,1)$ and obtained approximated series expressions of the first two eigenvalue curves $a(q)$ of the fractional Mathieu equation for small values of the parameter q.

There are several contributions in this paper that we consider relevant. First, we extend the analysis of the fractional Mathieu equation (2) presented in [12] by studying the behavior of the eigenvalue curves for $\alpha \in (0,2)$ and a much wider range of the parameter q. This more detailed analysis of the eigenvalue curves reveals the existence of degenerate eigenvalues of the fractional Mathieu equation which was not observed in [12], since the authors used a Fourier expansion of the solution with too few terms. A similar result has been observed for a fractional Ince equation [14]. We describe the properties of the fractional Mathieu functions (the solutions of (2)) in terms of periodicity and parity. Additionally, we discuss the characteristics of the degenerate solutions of the equation (corresponding to the degenerate eigenvalues).

Our analysis begins by analyzing the periodic solutions of Eq. (2) and the resulting matrix equations. We then illustrate the phenomenon of degeneracy in the eigenvalue curves. Finally we show some numerical examples of the solutions of the fractional Mathieu equation.

2. Solutions of the fractional Mathieu equation

We begin by recalling that the even and odd periodic solutions of the classical Mathieu equation (1) can be expanded in terms of Fourier series. The corresponding trigonometric expansions fall into four classes, according to their symmetry or antisymmetry, about $t = 0$ and $t = \pi/2$, namely [2]

$$\mathrm{ce}_{2n}(t;q) = \sum_{r=0}^{\infty} A_{2r}^{(2n)}(q)\cos 2rt, \tag{4a}$$

$$\mathrm{ce}_{2n+1}(t;q) = \sum_{r=0}^{\infty} A_{2r+1}^{(2n+1)}(q)\cos(2r+1)t, \tag{4b}$$

$$\mathrm{se}_{2n+1}(t;q) = \sum_{r=0}^{\infty} B_{2r+1}^{(2n+1)}(q)\sin(2r+1)t, \tag{4c}$$

$$\mathrm{se}_{2n+2}(t;q) = \sum_{r=0}^{\infty} B_{2r+2}^{(2n+2)}(q)\sin(2r+2)t, \tag{4d}$$

for $n = 0, 1, 2, \ldots$ To each family there belongs an infinite set of real eigenvalues, labeled a_{2n}, a_{2n+1}, b_{2n+1}, and b_{2n+2}, correspondingly. For $q > 0$ they follow the order $a_0 < b_1 < a_1 < b_2 < a_2 < \cdots$. Additionally, the Mathieu functions satisfy the following orthogonality properties [1]

$$\int_0^{2\pi} \mathrm{ce}_m(t;q)\mathrm{ce}_n(t;q)\mathrm{d}t = \int_0^{2\pi} \mathrm{se}_m(t;q)\mathrm{se}_n(t;q)\mathrm{d}t = \begin{cases} \pi, & \text{if } m = n \\ 0, & \text{if } m \neq n \end{cases}, \tag{5}$$

$$\int_0^{2\pi} \mathrm{ce}_m(t;q)\mathrm{se}_n(t;q)\mathrm{d}t = 0, \quad m, n \text{ positive integers.} \tag{6}$$

Equation (5) provides the normalization condition for the Fourier coefficients of the Mathieu functions, namely

$$2\{A_0^{(2n)}\}^2 + \sum_{r=1}^{\infty}\{A_{2r}^{(2n)}\}^2 = \sum_{r=1}^{\infty}\{A_{2r+1}^{(2n+1)}\}^2 = \sum_{r=1}^{\infty}\{B_{2r+1}^{(2n+1)}\}^2 = \sum_{r=1}^{\infty}\{B_{2r+2}^{(2n+2)}\}^2 = 1. \tag{7}$$

Our goal is to find periodic solutions of the fractional Mathieu equation (2). To do this, let us consider a solution in the form of a Fourier series of the form

$$\Theta(t;q) = A_0 + \sum_{r=1}^{\infty} A_r \cos rt + B_r \sin rt. \tag{8}$$

Note that $\Theta(t;q)$ can be periodic thanks to the choice $b = -\infty$ in Eq. (3). This is not the case for the standard choice of $b = 0$ (i.e. the initial time of the process, $t = 0$), which follows from the following theorem [15]:

Theorem 1 *Suppose that $f(t)$ is $(n-1)$-times continuously differentiable and $f^{(n)}(t)$ is bounded. If $f(t)$ is a non-constant periodic function with period T, the function ${}_0\mathrm{D}_t^{\alpha} f(t)$, where $0 < \alpha \notin \mathbb{N}$ and n is the first integer greater than α, cannot be a periodic function of period T.*

Corollary 1 *A differential equation of fractional order in the form*

$${}_0\mathrm{D}_t^{\alpha} f(t) + \Psi(f(t), f^1(t), ..., f^{(n)}(t)) = 0, \tag{9}$$

where $0 < \alpha \notin \mathbb{N}$, cannot have any non-constant smooth periodic solution.

To understand why this is the case, note that the Fourier series solution involves sine and cosine functions whose Riemann-Liouville fractional derivatives with lower limit $b = 0$ are non-periodic functions. They are given by [13]

$${}_0\mathrm{D}_t^{\alpha} \cos rt = (rt)^{-\alpha} E_{2,1-\alpha}(-r^2 t^2), \tag{10a}$$

$${}_0\mathrm{D}_t^{\alpha} \sin rt = (rt)^{1-\alpha} E_{2,2-\alpha}(-r^2 t^2), \tag{10b}$$

where $E_{\alpha,\beta}(z)$ is the two-parameter Mittag-Leffler function [13]

$$E_{\alpha,\beta}(z) = \sum_{k=0}^{\infty} \frac{z^k}{\Gamma(\alpha k + \beta)}, \qquad \begin{cases} \alpha > 0 \\ \beta > 0 \end{cases}. \tag{11}$$

Nevertheless, for large values of t, Eqs. (10) converge to the following periodic functions:

$${}_0\mathrm{D}_t^{\alpha} \cos rt = r^{\alpha} \cos(rt + \alpha\pi/2), \qquad t \to \infty, \tag{12a}$$

$${}_0\mathrm{D}_t^{\alpha} \sin rt = r^{\alpha} \sin(rt + \alpha\pi/2), \qquad t \to \infty. \tag{12b}$$

Mathematically, setting $b = -\infty$ in Eq. (3) leads to the same result, i.e.

$${}_{-\infty}\mathrm{D}_t^{\alpha} \cos rt = r^{\alpha} \cos(rt + \alpha\pi/2), \tag{13a}$$

$${}_{-\infty}\mathrm{D}_t^{\alpha} \sin rt = r^{\alpha} \sin(rt + \alpha\pi/2), \tag{13b}$$

$\alpha \in \mathbb{R}$. In more physical terms, the solutions are valid for the steady state of the system. Also, for this choice, the Riemann-Liouville and Caputo definitions of the fractional derivative are equivalent [13].

The Fourier solution (8) of the fractional Mathieu equation includes the four solutions (4) of the non-fractional Mathieu equation (1). Following the method of harmonic balance, we insert the series solution (8) into the fractional Mathieu equation (2) and collect terms to obtain the following recurrence relations:

$$aA_0 - qA_2 = 0, \tag{14a}$$

$$[a - 1 + q + c\cos(\alpha\pi/2)]B_1 - c\sin(\alpha\pi/2)A_1 - qB_3 = 0, \tag{14b}$$

$$c\sin(\alpha\pi/2)B_1 + [a - 1 - q + c\cos(\alpha\pi/2)]A_1 - qA_3 = 0, \tag{14c}$$

$$[a - 4 + c2^{\alpha}\cos(\alpha\pi/2)]B_2 - c2^{\alpha}\sin(\alpha\pi/2)A_2 - qB_4 = 0, \tag{14d}$$

$$-2qA_0 + c2^{\alpha}\sin(\alpha\pi/2)B_2 + [a - 4 + c2^{\alpha}\cos(\alpha\pi/2)]A_2 - qA_4 = 0. \tag{14e}$$

For $r > 3$,

$$-qB_{r-2} + [a - r^2 + cr^\alpha \cos(\alpha\pi/2)]B_r - cr^\alpha \sin(\alpha\pi/2)A_r - qB_{r+2} = 0, \tag{14f}$$
$$-qA_{r-2} + cr^\alpha \sin(\alpha\pi/2)B_r + [a - r^2 + cr^\alpha \cos(\alpha\pi/2)]A_r - qA_{r+2} = 0, \tag{14g}$$

where we used ${}_{-\infty}\mathrm{D}_t^\alpha A_0 = 0$ for $\alpha > 0$.

Note that these recurrence relation are now coupled in A_r and B_r. Additionally we can recognize two independent systems of equations, one involving only even subscripts (A_0, B_2, A_2,...) and the other involving odd subscripts (B_1, A_1, B_3,...). This means that there exist only two kinds of solutions, instead of four, as is the case of the classical Mathieu equation. The first solution is π-periodic, whereas the second is 2π-periodic, namely

$$\Theta_{2n}^{(\alpha)}(t;q) = A_0^{(2n)}(q) + \sum_{r=1}^{\infty} A_{2r}^{(2n)}(q)\cos 2rt + B_{2r}^{(2n)}(q)\sin 2rt, \tag{15a}$$
$$\Theta_{2n+1}^{(\alpha)}(t;q) = \sum_{r=0}^{\infty} A_{2r+1}^{(2n+1)}(q)\cos(2r+1)t + B_{2r+1}^{(2n+1)}(q)\sin(2r+1)t, \tag{15b}$$

where the order of the fractional derivative is indicated by the superscript (α). The eigenvalues of $\Theta_{2n}^{(\alpha)}(t;q)$ can be labeled as $a_{2n}^{(\alpha)}(q)$ and those of $\Theta_{2n+1}^{(\alpha)}(t;q)$ as $a_{2n+1}^{(\alpha)}(q)$. They follow the order $a_0 < a_2 < a_4$... and $a_1 < a_3 < a_5$..., respectively. Solutions (15) can be normalized in an analogous way as the Mathieu functions [Eqs. (7)].

3. Coefficient matrices and eigenvalue curves

Recurrence relations (14) may be written in matrix form in order to obtain the eigenvalue curves. Let M and N denote the coefficient matrices corresponding to the π- and 2π-periodic solutions of the fractional Mathieu equation, such that

$$M\Theta_{2n}^{(\alpha)} = a_{2n}^{(\alpha)}\Theta_{2n}^{(\alpha)}, \quad \text{and} \quad N\Theta_{2n+1}^{(\alpha)} = a_{2n+1}^{(\alpha)}\Theta_{2n+1}^{(\alpha)}, \tag{16}$$

i.e., they are the matrix representation of the fractional operator $[-\mathrm{d}^2/\mathrm{d}t^2 + 2q\cos 2t - c\,{}_{-\infty}\mathrm{D}_t^\alpha]$. By denoting $C \equiv c\cos(\alpha\pi/2)$ and $S \equiv c\sin(\alpha\pi/2)$ we get

$$M = \begin{pmatrix} 0 & 0 & \sqrt{2}q & 0 & 0 & 0 & 0 & \dots \\ 0 & 4-2^\alpha C & 2^\alpha S & q & 0 & 0 & 0 & \dots \\ \sqrt{2}q & -2^\alpha S & 4-2^\alpha C & 0 & q & 0 & 0 & \dots \\ 0 & q & 0 & 16-4^\alpha C & 4^\alpha S & q & 0 & \dots \\ 0 & 0 & q & -4^\alpha S & 16-4^\alpha C & 0 & q & \dots \\ \vdots & \vdots & \vdots & \vdots & \vdots & \vdots & \vdots & \ddots \end{pmatrix}, \tag{17}$$

$$N = \begin{pmatrix} 1-q-C & S & q & 0 & 0 & 0 & \dots \\ -S & 1+q-C & 0 & q & 0 & 0 & \dots \\ q & 0 & 9-3^\alpha C & 3^\alpha S & q & 0 & \dots \\ 0 & q & -3^\alpha S & 9-3^\alpha C & 0 & q & \dots \\ \vdots & \vdots & \vdots & \vdots & \vdots & \vdots & \ddots \end{pmatrix}. \tag{18}$$

The M matrix has the coefficients corresponding to A_0, B_2, A_2, B_4, A_4, ... on its columns, while the columns of the N matrix follow the order B_1, A_1, B_3, A_3, ... We can write one single

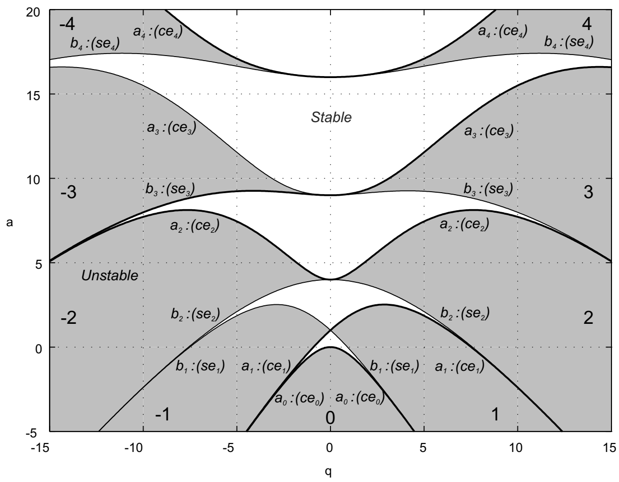

Figure 1. Eigenvalue curves of the standard Mathieu equation ($c = 0$) calculated with Eq. (8) using $r_{max} = 37$. Thick and thin lines denote curves for even $\mathrm{ce}(t; q)$ and odd $\mathrm{se}(t; q)$ Mathieu functions, respectively. The characteristic curves divide the plane into regions of stability (white) and instability (gray). The unstable regions are numbered sequentially for convenience.

matrix for all the coefficients, ordered as A_0, B_1, A_1, B_2, A_2, B_3, $A_3, \ldots$ The matrix equation takes the form

$$\begin{pmatrix} 0 & 0 & 0 & 0 & \sqrt{2}q & 0 & 0 & 0 & 0 & 0 & 0 & 0 & 0 & \ldots \\ 0 & 1-q-C & S & 0 & 0 & q & 0 & 0 & 0 & 0 & 0 & 0 & 0 & \ldots \\ 0 & -S & 1+q-C & 0 & 0 & 0 & q & 0 & 0 & 0 & 0 & 0 & 0 & \ldots \\ 0 & 0 & 0 & 4-2^\alpha C & 2^\alpha S & 0 & 0 & q & 0 & 0 & 0 & 0 & 0 & \ldots \\ \sqrt{2}q & 0 & 0 & -2^\alpha S & 4-2^\alpha C & 0 & 0 & 0 & q & 0 & 0 & 0 & 0 & \ldots \\ 0 & q & 0 & 0 & 0 & 9-3^\alpha C & 3^\alpha S & 0 & 0 & q & 0 & 0 & 0 & \ldots \\ 0 & 0 & q & 0 & 0 & -3^\alpha S & 9-3^\alpha C & 0 & 0 & 0 & q & 0 & 0 & \ldots \\ 0 & 0 & 0 & q & 0 & 0 & 0 & 16-4^\alpha C & 4^\alpha S & 0 & 0 & q & 0 & \ldots \\ 0 & 0 & 0 & 0 & q & 0 & 0 & -4^\alpha S & 16-4^\alpha C & 0 & 0 & 0 & q & \ldots \\ \vdots & \vdots & \vdots & \vdots & \vdots & \vdots & \vdots & \vdots & \vdots & \vdots & \vdots & \vdots & \vdots & \ddots \end{pmatrix} \begin{pmatrix} \sqrt{2}A_0 \\ B_1 \\ A_1 \\ B_2 \\ A_2 \\ B_3 \\ A_3 \\ B_4 \\ A_5 \\ \vdots \end{pmatrix} = a \begin{pmatrix} \sqrt{2}A_0 \\ B_1 \\ A_1 \\ B_2 \\ A_2 \\ B_3 \\ A_3 \\ B_4 \\ A_5 \\ \vdots \end{pmatrix}. \tag{19}$$

The coefficient matrix (19) depends on the values of c, α, and q. Fixing c and α, one can draw the curves $a(q)$ by calculating the eigenvalues of (19). The coefficients of the solutions (15) are the entries of the corresponding eigenvectors. Numerically, the matrix has to be truncated up to a certain dimension (the solutions (15) are truncated up to a given r_{max}) and then one can obtain its eigenvalues for a given domain of q.

To make suitable comparisons, in Fig. 1 we plot the known eigenvalue curves $a(q)$ and $b(q)$ for the non-fractional ($c = 0$) standard Mathieu equation [2]. The coefficient matrix in Eq. (19) becomes Hermitian, which results in it having an infinite set of real discrete eigenvalues and orthogonal eigenvectors. Thick and thin lines denote characteristic curves for even $\mathrm{ce}_m(t; q)$ and odd $\mathrm{se}_m(t; q)$ Mathieu functions, respectively. Even-order and odd-order curves are symmetrical and anti-symmetrical about the a-axis, respectively. Except for the trivial case $q = 0$, the curves do not intersect and thus divide the (q, a)-plane into regions where the solutions of the Mathieu equation Eq. (1) are stable (white regions) or unstable (gray regions). We have numbered the unstable regions for ease of reference, as shown in Fig. 1. Note that the j-th unstable region touches the axis $q = 0$ at values $a = |j|^2$.

The appearance of the fractional derivative gives rise to off-diagonal terms of the form $\pm r^\alpha S$ in the coefficient matrix Eq. (19), making it non-Hermitian. Thus, for nonzero c and α one cannot expect its eigenvalues to be all real nor its eigenvectors to be orthogonal. In Fig. 2 we

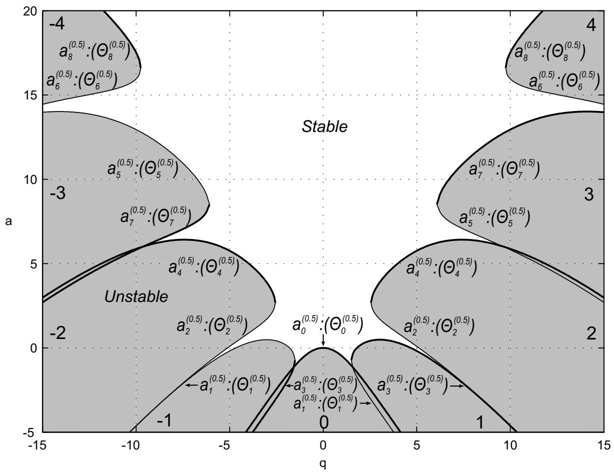

Figure 2. Eigenvalue curves of the fractional Mathieu equation ($c = 2$, $\alpha = 0.5$) calculated with Eq. (8) using $r_{max} = 37$. Cross points of the curves represent degenerate eigenvalues of the fractional Mathieu equation. Unstable regions are numbered sequentially starting from the lowest curve.

plotted the eigenvalue curves $a(q)$ for the fractional Mathieu equation with $c = 2$ and $\alpha = 0.5$. Once again the curves divide the (q, a)-plane into regions where the solutions of the fractional Mathieu equation are stable (white region) or unstable (gray region). The unstable regions are numbered sequentially following the same convention as in Fig. 1. In general for $c > 0$ and $\alpha \in (0, 1)$ we observe the following:

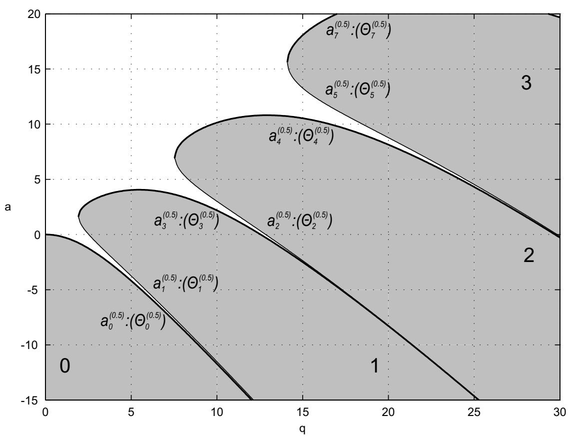

Figure 3. Eigenvalue curves of the fractional Mathieu equation ($c = 2$, $\alpha = 1.3$) calculated with a truncated solution [Eq. (8)] using $r_{max} = 37$. The curves, unlike the case $\alpha \in (0, 1)$, no longer cross.

- Except for the lowest-order curve $a_0(q)$, each eigenvalue curve of the fractional Mathieu equation becomes "detached" from the a-axis. The upper and lower boundaries of the unstable regions correspond to the original curves $a(q)$ and $b(q)$ of the standard Mathieu equation and are depicted using different line-widths in Fig. 2.
- The upper and lower eigenvalue curves of an unstable region connect smoothly, forming a single continuous boundary-curve. For $q > 0$, the *turning-point* of the boundary-curve is

the minimum value of q for which the eigenvalue a is real. For each boundary-curve, the solutions above and below of the turning-points are labeled with different subindexes.

- Mathieu solutions corresponding to different points (q, a) lying on the same boundary-curve have the same periodicity, namely, π and 2π for boundary-curves of even and odd unstable regions, respectively.
- For a given q, there is only a finite number of real eigenvalues, which increases as q increases. Consequently, unlike the classical Mathieu equation, the fractional Mathieu equation has a finite number of real periodic solutions for a given value of q.
- In the "detached" (stable) region, the eigenvalues become complex, and they appear in complex conjugate pairs (i.e. $a^{(\alpha)}_{2n+1} = \overline{a}^{(\alpha)}_{2n+3}$ and $a^{(\alpha)}_{2n+2} = \overline{a}^{(\alpha)}_{2n+4}$, n even).
- There exist real values q^* where the eigenvalue curves intersect, indicating the existence of degenerate eigenvalues or *double points* of the fractional Mathieu equation. In particular, the crossings occur for all pairs of curves $\{a^{(\alpha)}_{2n}, a^{(\alpha)}_{2n+1}\}$ when $q > 0$, and for the curves $\{a^{(\alpha)}_{4n}, a^{(\alpha)}_{4n+2}\}$ and $\{a^{(\alpha)}_{4n+1}, a^{(\alpha)}_{4n+3}\}$ when $q < 0$. Incidentally, it is known that the classical Mathieu equation (1) exhibits double eigenvalues for complex values of q. (See [16, 17] for the case of purely imaginary q.)
- The adjacent curves become asymptotically parallel after the crossing, therefore they only cross once.

For $\alpha \in [1, 2]$, the eigenvalue curves no longer cross and thus there are no degenerate eigenvalues, as shown in Fig. 3. As expected, when $\alpha = 2$, we recover the standard Mathieu equation scaled by a factor $1 + c$, and the curves become "reattached", as shown in Fig. 1.

4. Behavior of the fractional Mathieu functions

The behavior of the solutions of the fractional Mathieu equation 2 is fairly complicated, particularly because we have to understand the dependence of the functions on the variable t and the parameters q and c and the fractional-order α. Let us consider first the effect of varying the order of the fractional derivative term. The behavior of the normalized fractional solution $\Theta^{(\alpha)}_3(t, 2)$ with $c = 1$ and $q = 2$ as a function of t is depicted in Fig. 4 for the range $\alpha \in [0, 2]$. Solid curves correspond to $\alpha = \{0, 0.5, 1, 1.5, 2\}$. When α vanishes, the fractional Mathieu equation reduces to the standard Mathieu equation and $\Theta^{(\alpha)}_3(t; q)$ becomes $\mathrm{ce}_1(t; q)$. Similarly, when $\alpha = 2$, the fractional Mathieu equation reduces to a scaled version of the standard Mathieu equation and $\Theta^{(\alpha)}_3(t; q)$ now becomes $\mathrm{ce}_1(t; q/(1 + c))$. In this way, the Mathieu functions $\mathrm{ce}_1(t; q)$ and $\mathrm{ce}_1(t; q/(1 + c))$ have been smoothly connected by varying the order of the fractional term of the fractional Mathieu equation. Note that whereas the even and odd integer-order Mathieu functions are symmetrical and antisymmetrical about the origin, respectively, the fractional solutions (i.e. $\alpha \neq 0, 2$) do not have a definite parity.

Unlike the Mathieu functions, two solutions of the fractional Mathieu equation belonging to the same family (Eqs. (15a) or (15b)) with different eigenvalues a are not orthogonal for a given q. This can be observed by letting Θ_m and Θ_n (omitting the superscript α) be two solutions of the same family (π- or 2π-periodic) with equal q and different eigenvalues a_m, a_n. By writing $\mathrm{D}^\alpha \equiv {}_{-\infty}\mathrm{D}^\alpha_t$ the solutions satisfy the equations

$$\Theta''_m + (a_m - 2q\cos 2t)\Theta_m + c\mathrm{D}^\alpha\Theta_m = 0, \tag{20a}$$

$$\Theta''_n + (a_n - 2q\cos 2t)\Theta_n + c\mathrm{D}^\alpha\Theta_n = 0. \tag{20b}$$

Multiplying the first equation by Θ_n and the second equation by Θ_m and subtracting both, we get

$$\Theta''_m\Theta_n - \Theta''_n\Theta_m = (a_n - a_m)\Theta_m\Theta_n + c[\Theta_m\mathrm{D}^\alpha\Theta_n - \Theta_n\mathrm{D}^\alpha\Theta_m]. \tag{21}$$

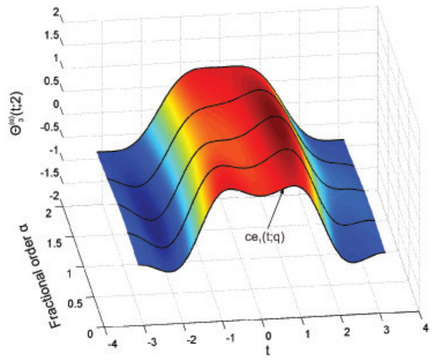

Figure 4. $\Theta_3^{(\alpha)}(t;2)$ solution of the fractional Mathieu equation for $\alpha \in [0,2]$. Solid curves correspond to $\alpha = \{0, 0.5, 1, 1.5, 2\}$.

Integrating both sides between t_1 and t_2, we get, after integrating by parts the LHS

$$[\Theta'_m\Theta_n - \Theta'_n\Theta_m]_{t_1}^{t_2} = (a_n - a_m)\int_{t_1}^{t_2}\Theta_m\Theta_n\mathrm{d}t + c\int_{t_1}^{t_2}[\Theta_m\mathrm{D}^\alpha\Theta_n - \Theta_n\mathrm{D}^\alpha\Theta_m]\mathrm{d}t. \tag{22}$$

Since the Θ solutions are π- or 2π-periodic, we set $t_1 = 0$ and $t_2 = 2\pi$, so that the LHS vanishes, and we obtain

$$(a_n - a_m)\int_0^{2\pi}\Theta_m\Theta_n\mathrm{d}t + c\int_0^{2\pi}[\Theta_m\mathrm{D}^\alpha\Theta_n - \Theta_n\mathrm{D}^\alpha\Theta_m]\mathrm{d}t = 0. \tag{23}$$

In the case $c = 0$ (or $\alpha = 0$), this shows that two functions of the same family with different eigenvalues are orthogonal. We can show by direct substitution that the second member of the LHS does not vanish. Take, for example, two solutions of the 2π-periodic family, say

$$\Theta_m(t;q) = \sum_{r=1,3,\ldots}^{\infty} A_r^{(m)}\cos rt + B_r^{(m)}\sin rt, \tag{24}$$

$$\Theta_n(t;q) = \sum_{r=1,3,\ldots}^{\infty} A_r^{(n)}\cos rt + B_r^{(n)}\sin rt. \tag{25}$$

For this case, we have

$$\int_0^{2\pi}[\Theta_m\mathrm{D}^\alpha\Theta_n - \Theta_n\mathrm{D}^\alpha\Theta_m]\mathrm{d}t = 2\pi\sin(\alpha\pi/2)\sum_{r=1,3,\ldots}^{\infty} r^\alpha[A_r^{(n)}B_r^{(m)} - A_r^{(m)}B_r^{(n)}], \tag{26}$$

$$\neq 0, \tag{27}$$

which means

$$\int_0^{2\pi}\Theta_m\Theta_n\mathrm{d}t \neq 0. \tag{28}$$

Therefore, in general $\Theta_m^{(\alpha)}(t;q)$ and $\Theta_n^{(\alpha)}(t;q)$ are not orthogonal.

5. Behavior of degenerate solutions of the fractional Mathieu equation

Since the fractional Mathieu equation has a periodic solution for each point (q, a) lying on the eigenvalue curves in Fig. 2, the cross-points between adjacent curves define degenerate Mathieu

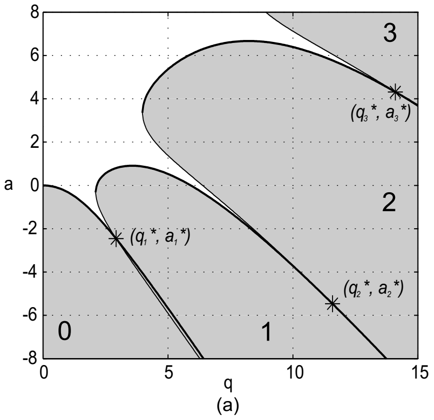

Crossing points

	q_i^*	a_i^*
i=1	2.9314097325	-2.4665599008
i=2	11.5799970244	-5.4592974346
i=3	14.1259933909	4.2988418885

(b)

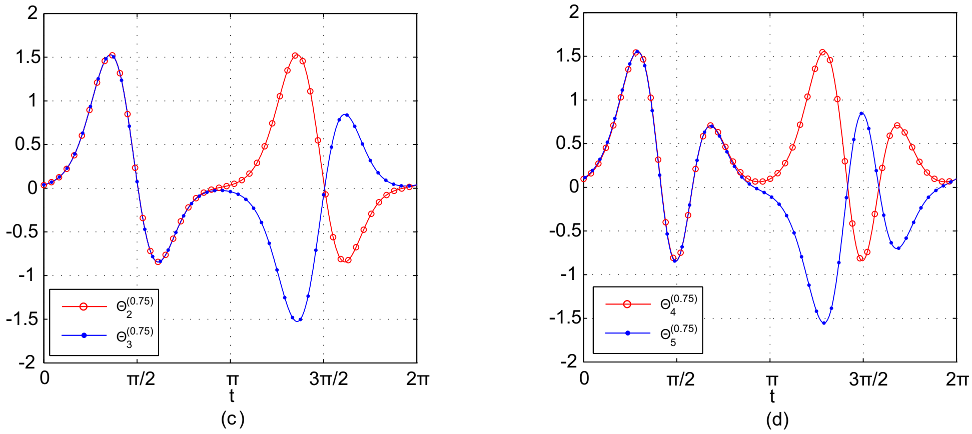

Figure 5. (a) (b) The first three eigenvalue curves and its corresponding cross-points for the fractional Mathieu equation with $c = 2$, $\alpha = 0.75$. (c) (d) Degenerate fractional Mathieu functions for the pairs (q_2^*, a_2^*) and (q_3^*, a_3^*).

solutions with the same values of q and a. Let us illustrate the behavior of the degenerate solutions. Figure 5(a) shows the first three eigenvalue curves $a(q)$ for $\alpha = 0.75$ and $c = 2$. The crossing points locating the degenerate eigenvalues are marked with asterisks on the curves and their numerical values are given up to ten decimals of precision in Fig. 5(b). Explicitly we have

$$a_0^{(\alpha)}(q_1^*) = a_1^{(\alpha)}(q_1^*), \qquad a_2^{(\alpha)}(q_2^*) = a_3^{(\alpha)}(q_2^*), \qquad a_4^{(\alpha)}(q_3^*) = a_5^{(\alpha)}(q_3^*). \tag{29}$$

The solutions can be easily plotted once the eigenvectors of matrices (17) and (18) have been calculated.

The behavior of the second and third pairs of degenerate fractional Mathieu functions is depicted in Figs. 5(c) and 5(d). Consider, for instance, the pair (q_2^*, a_2^*). The degenerate functions $\Theta_2^{(0.75)}(t; q_2^*)$ and $\Theta_3^{(0.75)}(t; q_2^*)$ satisfy the same differential equation, namely

$$\left[\frac{\mathrm{d}^2}{\mathrm{d}t^2} + a_2^* - 2q_2^* \cos 2t + 2\,{}_{-\infty}\mathrm{D}_t^{0.75}\right] \Theta^{(0.75)}(t; q_2^*) = 0. \tag{30}$$

Note that the even-order functions (red-circle lines) are π-periodic whereas odd-order functions (blue-point lines) are 2π-periodic. In general, in any pair of degenerate solutions one of them has period π and the other 2π. In particular, the π-periodic functions (red-circle lines) shown in Figs. 5(c) and 5(d) belong to the same boundary-curve of the second unstable region.

6. Conclusions

This work extends the analysis given in [12] concerning the solutions and the eigenvalue curves of the fractional Mathieu equation. The matrix form of the problem indicates that only two families of solutions exist, unlike the ordinary Mathieu equation. These solutions, valid for the steady state of the system to be studied, are not orthogonal and have no defined parity. We showed the appearance of degenerate eigenvalues for $c > 0$, $\alpha \in (0, 1)$ (seen as cross-points of the eigenvalue curves), which had not been observed in the previous treatment of the fractional Mathieu equation. This gives rise to new questions regarding the stability of the solutions in the overlapping regions on the (q, a)-plane.

Acknowledgements
This research was supported by Consejo Nacional de Ciencia y Tecnologia Mexico (Grant No. 82407) and by Tecnologico de Monterrey.

References

[1] Arscott F M 1964 *Periodic Differential Equations* (London: Pergamon Press)
[2] McLachlan N W 1951 *Theory and Application of Mathieu Functions* (Oxford: Clarendon Press)
[3] Gutiérrez-Vega JC, Rodríguez-Dagnino RM, Meneses-Nava MA, and Chávez-Cerda S 2003 Mathieu functions, a visual approach *Am J Phys* **71** 233–42
[4] Taylor J H, Narendra K S 1969 Stability regions for the damped Mathieu equation *SIAM J Appl Math* **17**, 343–52
[5] Richards J A 1976 Stability diagram approximation for the lossy Mathieu equation *SIAM J Appl Math* **30** 240–47
[6] Ramani D V, Rand R H and Keith W L 2001 Perturbation solution for bifurcation in the quadratically damped Mathieu equation *Proceedings of the 2001 ASME Design Engineering Technical Conferences* (Pittsburgh, PA)
[7] Gunderson H, Rigas H, VanVleck F S 1974 A technique for determining stability regions for the damped Mathieu equation *SIAM J Appl Math* **26** 345–49
[8] El-Dib Y O 2001 Nonlinear Mathieu equation and coupled resonance mechanism *Chaos, Solitons & Fractals* **12** 705–20
[9] Ng L, Rand R H 2002 Bifurcations in a Mathieu equation with cubic nonlinearities *Chaos, Solitons & Fractals* **14** 173–81
[10] Zounes R S, Rand R H 1998 Transition curves for the quasi-periodic Mathieu equation *SIAM J Appl Math* **58** 1094–115
[11] Insperger T, Stépán G 2002 Stability chart for the delayed Mathieu equation *Proceedings: Mathematical, Physical and Engineering Sciences* **458** 1989–98
[12] Rand RH, Sah SM, Suchorsky MK 2010 Fractional Mathieu equation *Commun Nonlinear Sci Numer Simulat* **15** 3254–62
[13] Podlubny I 1990 *Fractional Differential Equations* (San Diego: Academic Press)
[14] Parra Hinojosa A, Gutiérrez Vega J C 2013 Fractional Ince equation with a Riemann–Liouville fractional derivative. Applied Mathematics and Computation **219** 10695–705
[15] Tavazoei M S 2010 A note on fractional-order derivatives of periodic functions *Automatica* **46** 945–48
[16] Blanch G, Clemm D S 1969 The double points of Mathieu's differential equation *Math Comp* **23** 97–108
[17] Shivakumar P N, Xue J 1999 On the double points of a Mathieu equation *J Comput Appl Math* **107** 111–25